X-rays from laser produced plasmas

Danilo Giulietti [1, 2] & ***Alessandro Curcio*** [2]

[1] *Physics Department of the University and INFN, Pisa, Italy*

[2] *Laboratori Nazionali di Frascati, INFN, Frascati, Roma, Italy*

UNIVERSITÀ DI PISA

Istituto Nazionale di Fisica Nucleare

danilo.giulietti@unipi.it

SUMMARY

Since the early 60s, with the advent of LASERs, it was understood how they could be used to create pulsed X-ray sources of extraordinary brightness, by **directly focusing the radiation on a solid target**. The peculiar characteristics of these sources have progressively been implemented hand in hand with the evolution of laser technologies. In fact, as the duration of the laser pulses became shorter and consequently higher intensities were reached, denser and hotter plasmas were produced, with a consequent increase in the source brightness and energy of the emitted photons. With the **further advent of the amplification techniques of ultrashort laser pulses (fs)** and the overwhelming development of the **acceleration of high energy electrons (GeV) in laser produced plasmas**, new possibilities of generating X-rays have become possible. Among these the most important are (a) **the bremsstrahlung radiation**, produced by directing the high energy electrons on high atomic number targets (b) the **betatron radiation** produced by the accelerated electrons in the plasma, during their transverse oscillation motion as they propagate at relativistic speeds in the low-density channel induced by the laser pulse via the ponderomotive forces.

danilo.giulietti@unipi.it

Laser-Matter Interaction

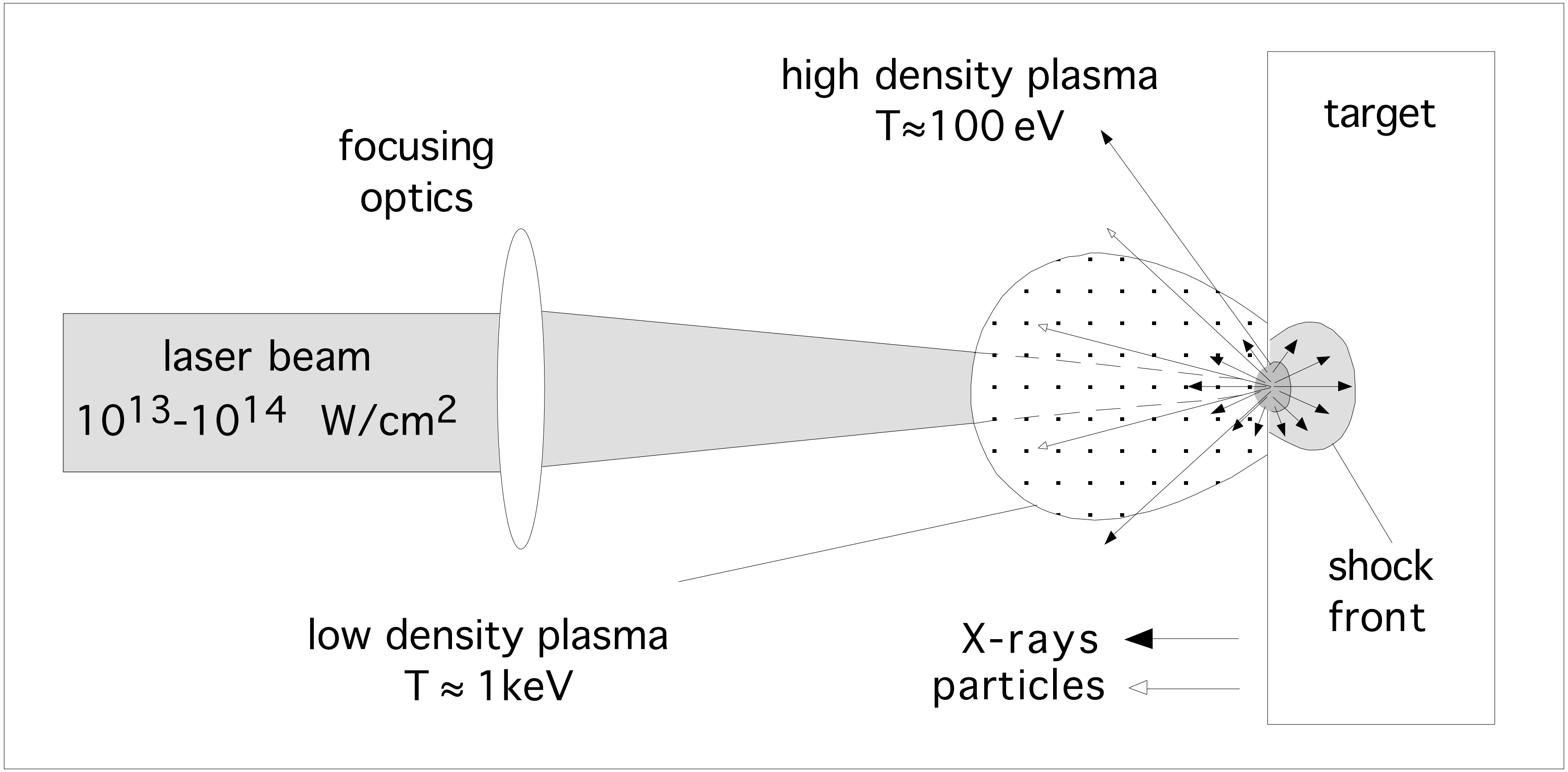

Black-body versus plasma emission

$$metal \qquad \lambda_{max} = \frac{2660}{T_K}\mu = \frac{2300}{T_{eV}}\mathring{A}$$

$$blackbody \qquad \lambda_{max} = \frac{2900}{T_K}\mu = \frac{2500}{T_{eV}}\mathring{A}$$

$$plasma \qquad \lambda_{max} = \frac{7200}{T_K} = \frac{6200}{T_{eV}}\mathring{A}$$

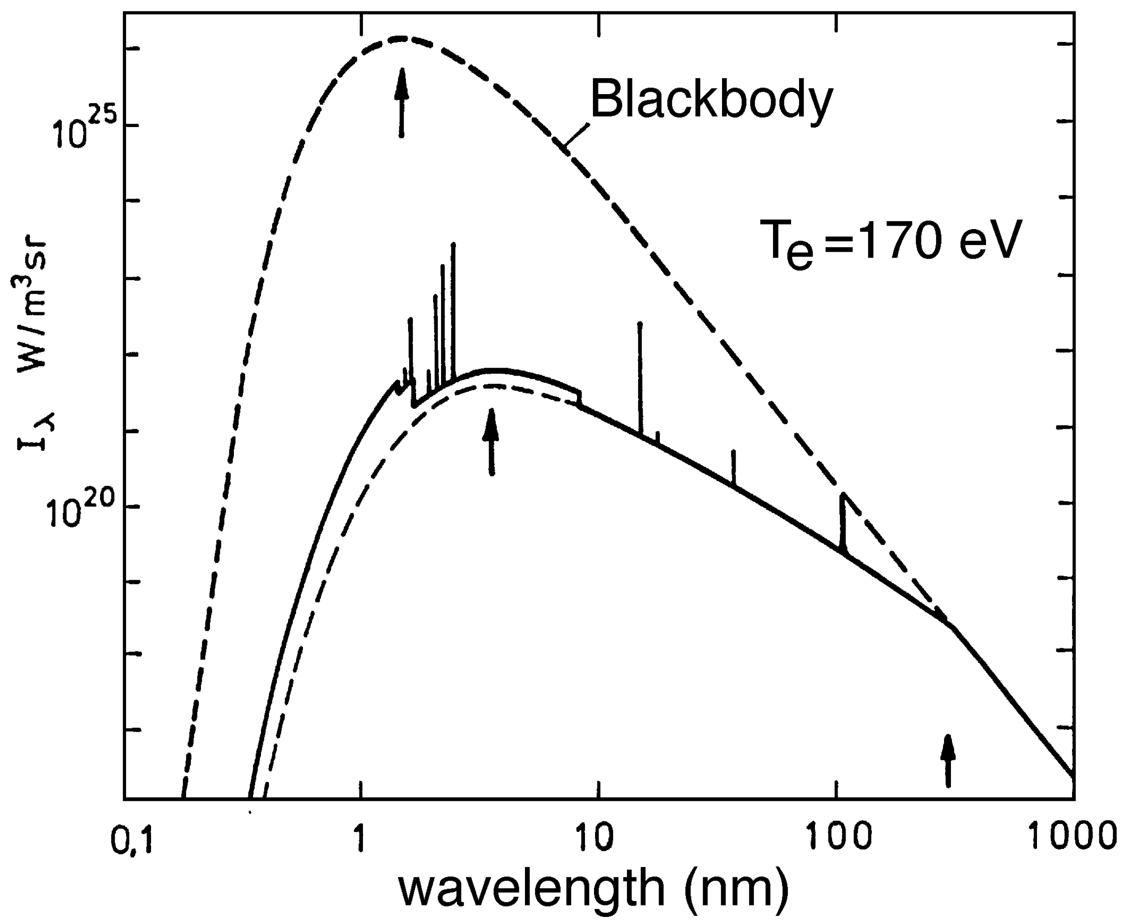

Focusing on solid target

LASER: 100J in 1ns, focal spot $\phi \approx 100\mu m$

$B_x \approx 10^{13}$ W cm^{-2} $strad^{-1}$

LASER: 10J in 20fs, focal spot $\phi \approx 100\mu m$

$B_x \approx 10^{17}$ W cm^{-2} $strad^{-1}$

LASER-PLASMA ACCELERATION

LASER PLASMA ACCELERATION (1)

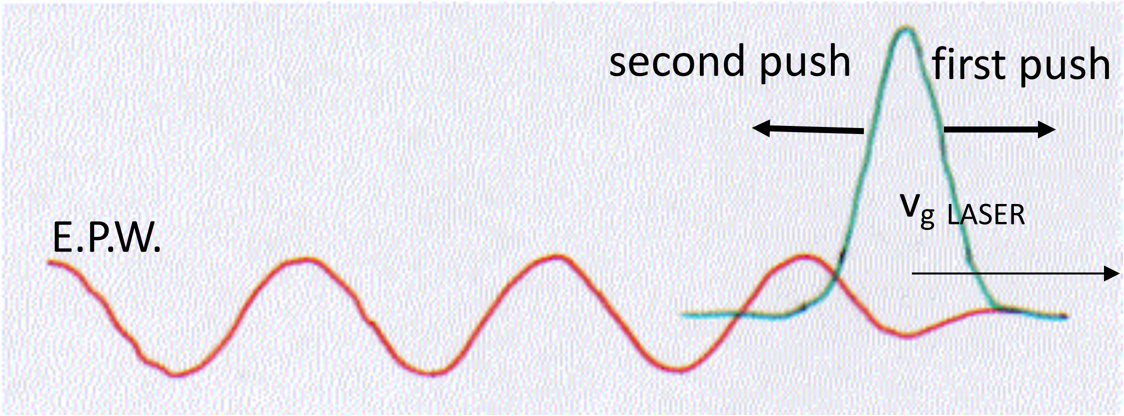

$$\tau \cdot c \approx \frac{\lambda_p}{2} \Leftrightarrow \tau \approx \frac{T_p}{2} \Rightarrow n_e\left(cm^{-3}\right) \approx \frac{3 \cdot 10^{-9}}{\tau_{(s)}^2}$$

$$example : \tau = 30\, fs \Rightarrow n_e \approx 3.3 \cdot 10^{18}\, cm^{-3}$$

$$v_{\phi,epw} = v_{g,laser} = c\left[1 - \frac{\omega_{pe}^2}{\omega^2}\right]^{\frac{1}{2}}$$

danilo.giulietti@unipi.it

LASER PLASMA ACCELERATION (2)

$$for\ \gamma_p \approx \frac{\omega}{\omega_{pe}} >> 1 \ \Rightarrow \ \Delta W_{\max} = 4\gamma_p^2 \frac{\delta n_e}{n_e} mc^2$$

$$energy\ gain\ \ along\ \ L_{deph} \approx \gamma_p^2 \lambda_p \ , \qquad \lambda_p \approx \frac{2\pi c}{\omega_{pe}}$$

$$\Delta W_{\max} \approx eE_{\max} \cdot L_{deph} \propto n_e^{\frac{1}{2}} \cdot \frac{1}{n_e} \cdot n_e^{-\frac{1}{2}} = \frac{1}{n_e}$$

PLASMONX
Electron LASER-Plasma Acceleration@LNF

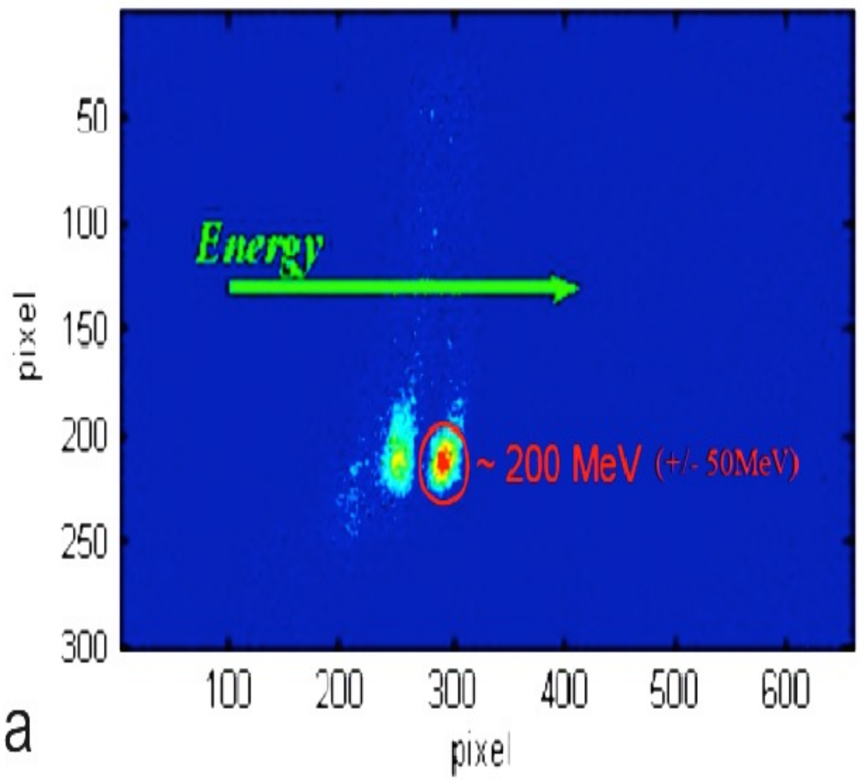

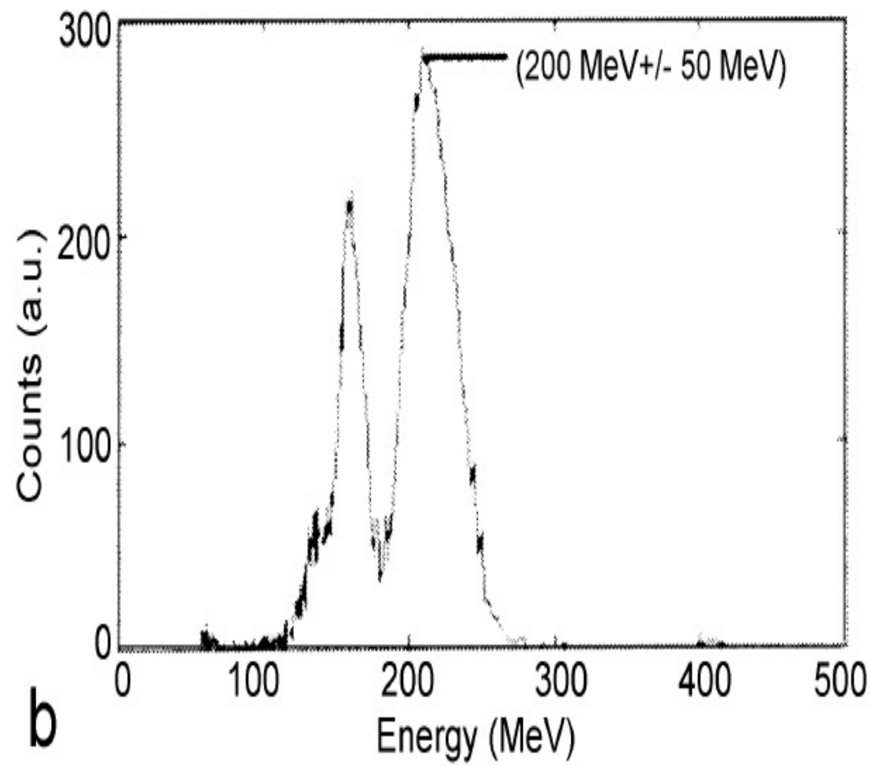

SPECTRUM OF ACCELERATED ELECTRONS

10mm He gas-jet
n_e= 1-4x10^{19} cm^{-3}
λ_L=0.815 µm
I_0=2x10^{19}Wcm^{-2}

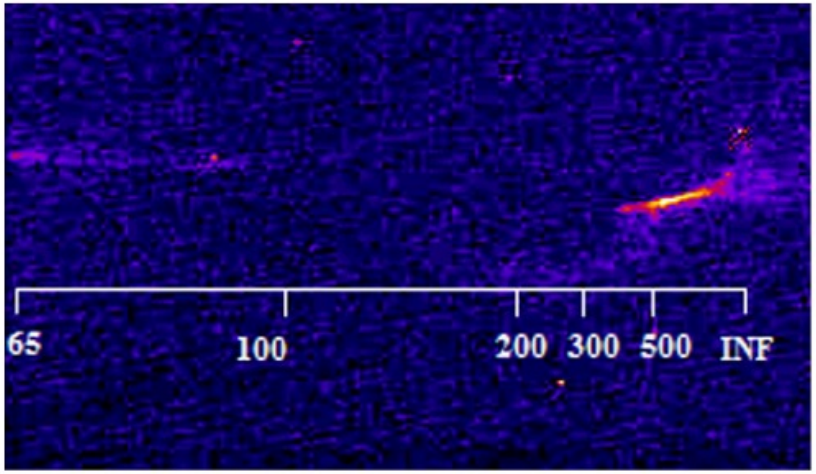

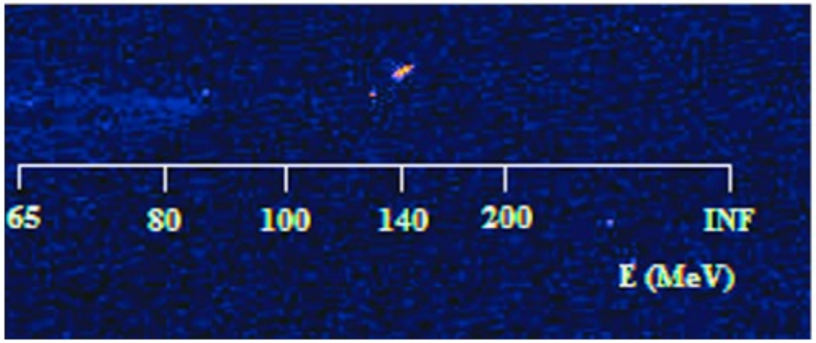

Fig. 6. Upper image: Electron spectrum obtained at 8 bars, showing a cut-off energy above 450 MeV (see text). Lower image: Electron spectrum obtained showing the lowest energy spread (4.6 %), obtained again at 8 bars.

SECONDARY SOURCES

- Energetic electrons on high Z solid target
- Betatron radiation
- Thomson Scattering
- FEL

Energetic electrons on high Z solid target

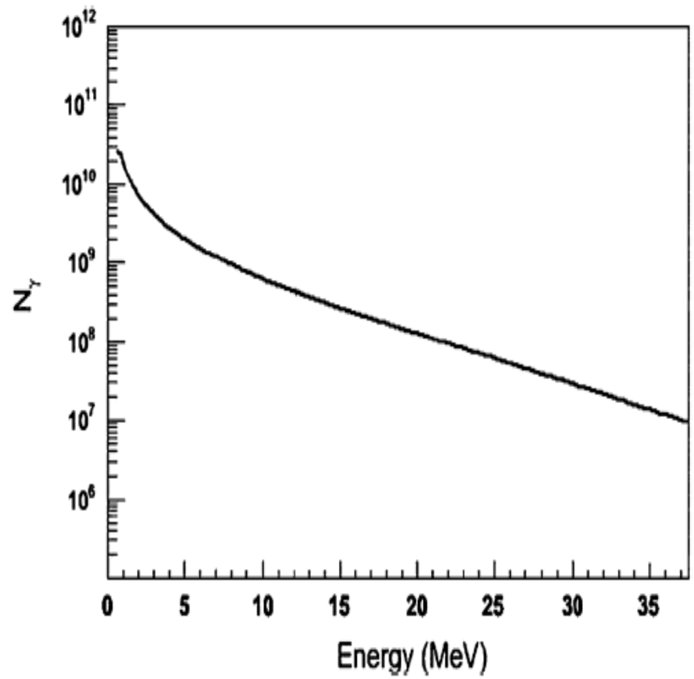

FIG. 3. Spectrum of the γ radiation produced by the electron bunches crossing the 2 mm tantalum slab, as calculated from the postprocessing activity measurements.

A. Giulietti, D. Giulietti et al, Intense γ-Ray Source in the Giant-Dipole-Resonance Range Driven by 10-TW Laser Pulses,Phys. Rev. Lett. 101, 105002, 2008

BETATRON RADIATION

LASER PLASMA ACCELERATION

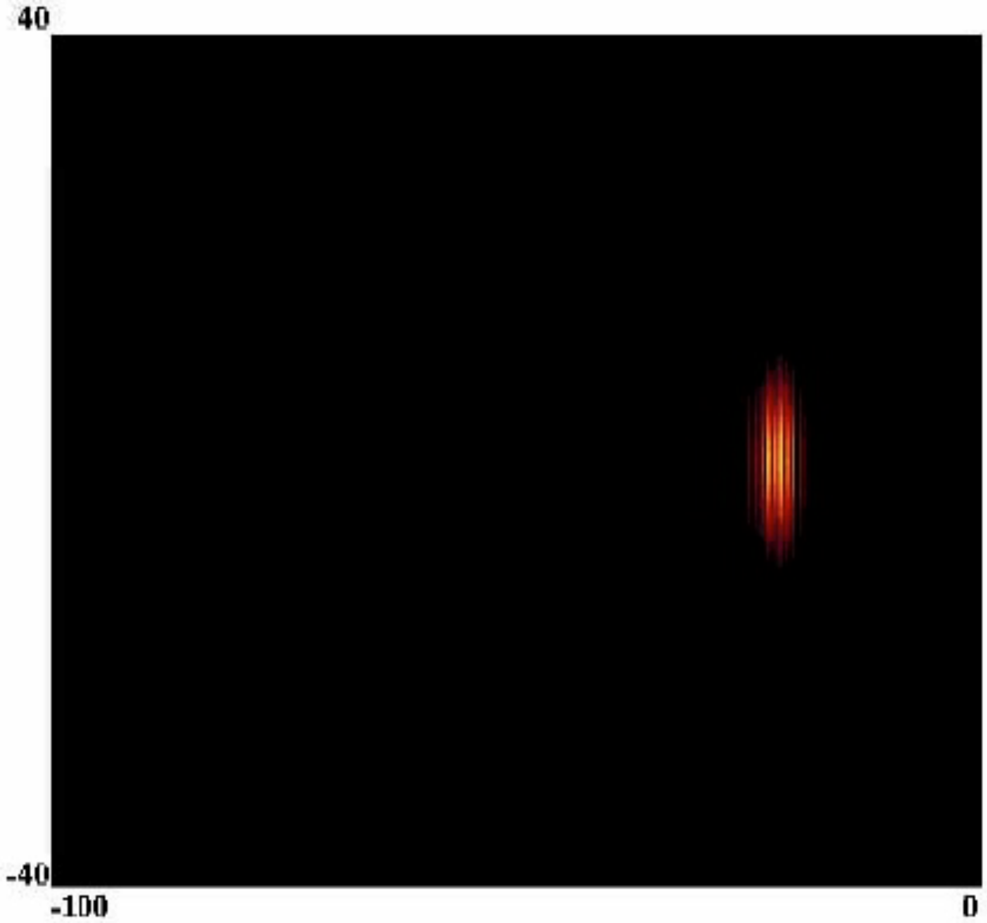

PIC simulation by Carlo Benedetti, INFN-BO

$N_e = 10^{19} cm^{-3}$

$L = 1mm$

$T = 20fs$

$W = 9\mu m$

$I = 1.5\ 10^{20} W/cm^2$

$U_{el} \approx 400MeV$

Bubble regime

danilo.giulietti@unipi.it

Principles of the Betatron radiation

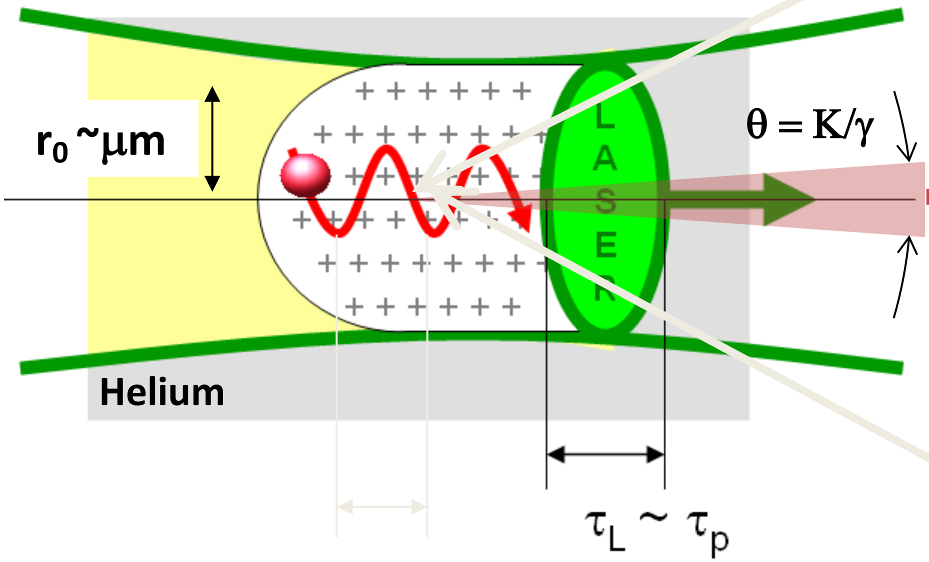

Plasma accelerator

Acceleration field
~ TeV / meter

$E_L \rightarrow$ 200 MeV

X-ray beam:

10^9 ph/shot
20 mrad
femtosecond

Plasma wiggler

λ_u ~ 100 µm

***K* ~ 20>1,wiggler**

$K = \gamma k_b r_0$

λ_u ~ 100 µm

Betatron oscillation

K ~ $\gamma r_0/\lambda_{bet.}$

A. Rousse et al., Phys. Rev. Lett 93, 135005(2004)

Courtesy V. Malka

Betatron radiation

Electron plasma density $10^{18}/cm^3$, laser pulse $20 - 40fs$

Laser pulse energy $E_l = 6J$*, Electron bunch charge* $Q_B = 100pC$
Diameter of the laser focal spot $\sim 10\mu m$
Electron initial configuration space : back of the bubble
Acceleration length $\sim$ *Dephasing length* ~ 11 *mm*
Pump depletion length ~ 11 *mm*

Betatron spectrum
$n_e = 1.8 \times 10^{18}/cm^3$, $\gamma_{max} \sim 3200$,
$\tau = 40fs$

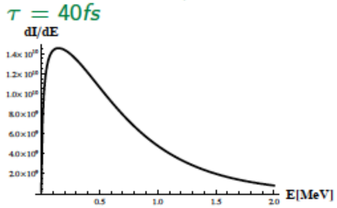

Critical energy $E_c \sim 600$ keV
Spatial distribution of the radiation collected at 1 meter

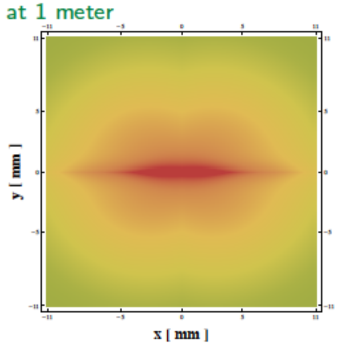

Laser polarization along x
Red stands for ~ 7 $\mu J/mm^2$

Betatron spectrum
$n_e = 1.8 \times 10^{19}/cm^3$, $\gamma_{max} \sim 4200$,
$\tau = 20fs$

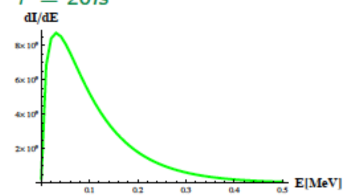

Critical energy $E_c \sim 120$ keV
Spatial distribution of the radiation collected at 1 meter

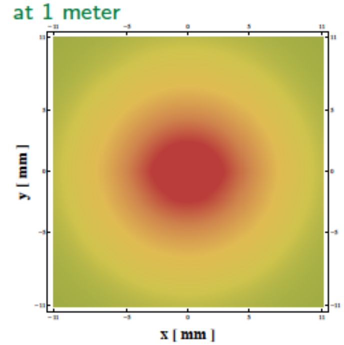

Laser polarization along x
Red stands for ~ 0.5 mJ/mm^2

danilo.giulietti@unipi.it

Thomson Scattering

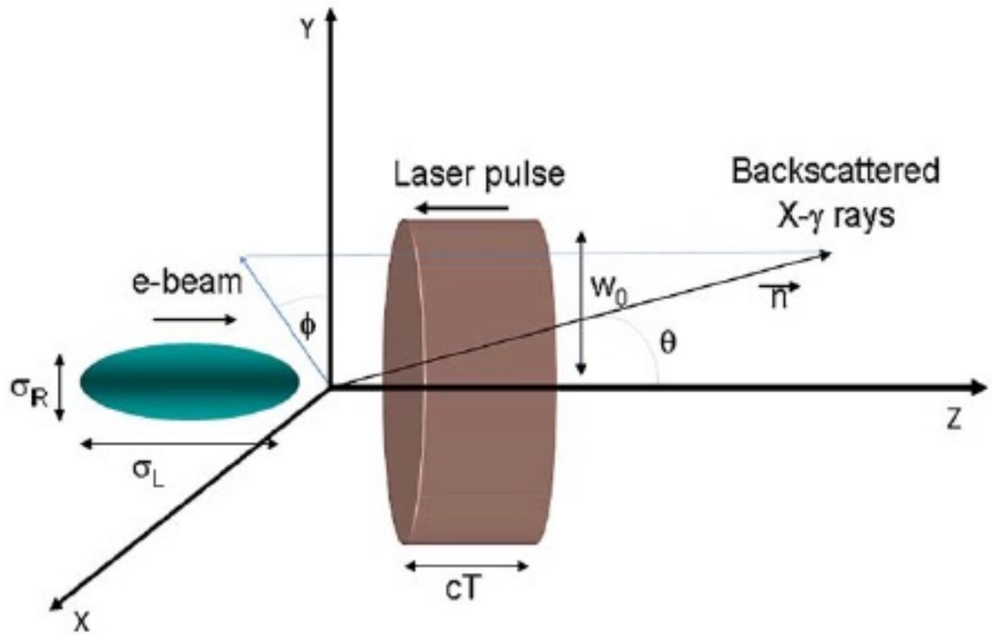

Fig. 1. Thomson backscattering geometry. The electron beam of longitudinal and transverse size σ_L and σ_R, respectively, is moving at a relativistic speed from left to right, colliding with a photon beam of waist size w_0 and duration T, thus emitting scattered radiation mainly in the direction of motion of the electron beam.

Start-to-end simulation of a Thomson source for mammography, P. Oliva, ….D. Giulietti et al, NIM A, **615**, 93-99, 2010

THOMSON BACK-SCATTERING

$$\nu_T = \nu_0 \frac{1-\beta\cos\alpha_L}{1-\beta\cos\theta} \approx \nu_0 \frac{4\gamma^2}{1+\theta^2\gamma^2} \approx 4\gamma^2\nu_0$$

$$for \quad \alpha_L = \pi \quad and \quad \theta << 1 \quad or \quad \theta = 0$$

$\longrightarrow$

e^- (30MeV); λ_0=1μm, E_0=1.24 eV $\longrightarrow$ λ_T=0.069 x10^{-8}nm, E_T=18 KeV

e^- (200 MeV); λ_0=1μm, E_0=1.24 eV λ_T=1.56 x10^{-3} nm, E_T=800 KeV

Spectral-angular distribution

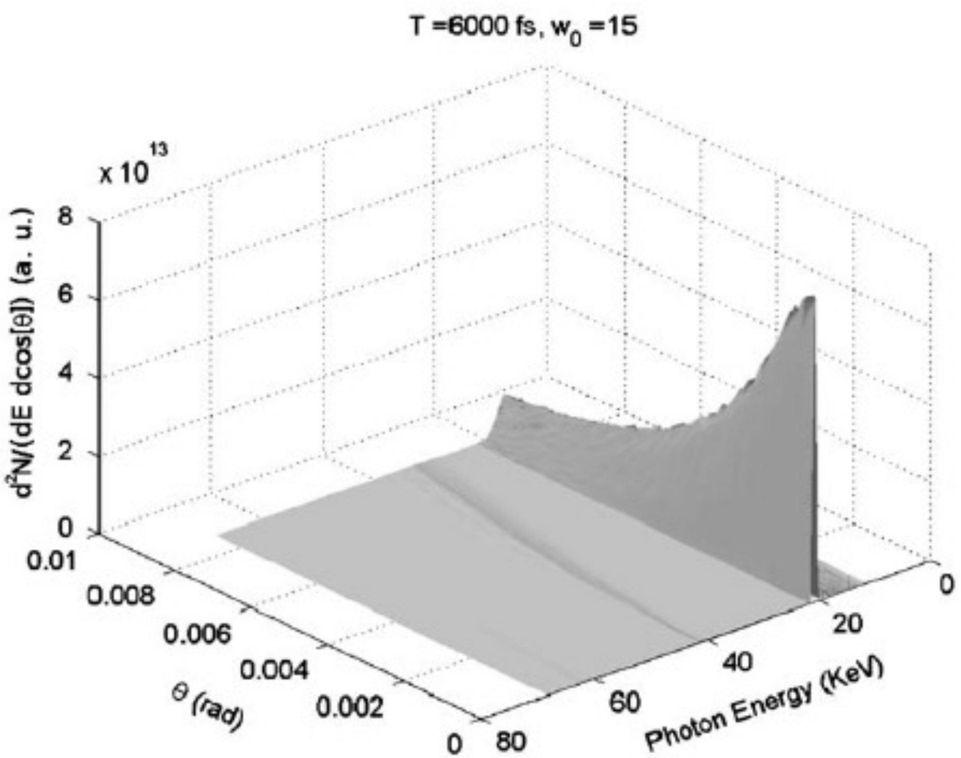

Fig. 8. Spectral-angular (integrated in the azimuthal angle ϕ) distribution of the collected radiation for the optimized parameters w_0=15 µm and duration T=6ps, ϑ_M=8 mrad.

FREE ELECTRON LASER

danilo.giulietti@unipi.it

UNDULATOR

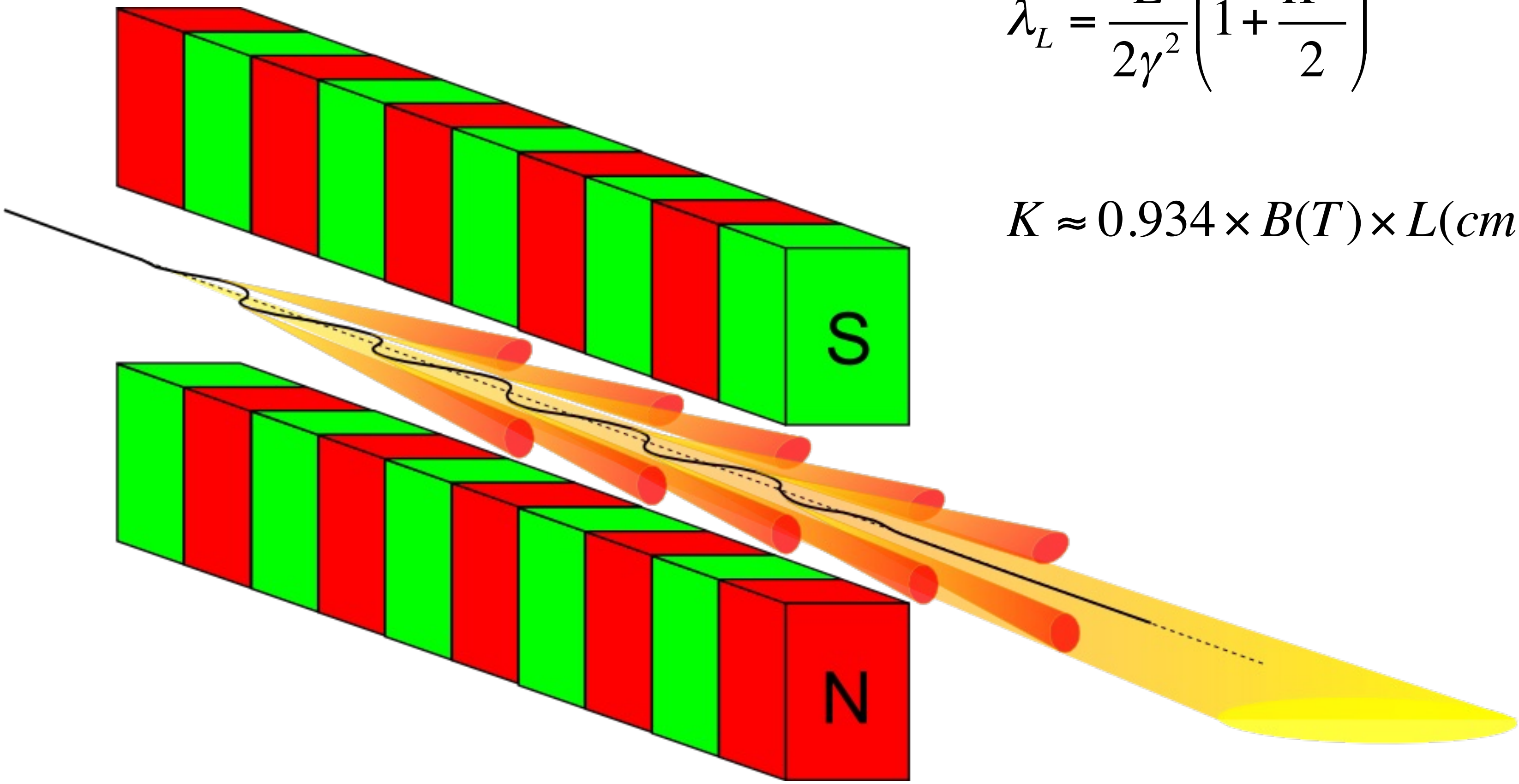

$$\lambda_L = \frac{L}{2\gamma^2}\left(1+\frac{K^2}{2}\right)$$

$$K \approx 0.934 \times B(T) \times L(cm)$$

danilo.giulietti@unipi.it

ENEA UNDULATOR

danilo.giulietti@unipi.it

CONCLUSIONS

We certainly cannot ignore the most important sources of X-ray radiation available at LINACs or synchrotrons, nor the quality of that radiation in terms of tunability, energy spread and divergence. However, the sources of X-ray radiation from laser produced plasmas undoubtedly remain favorable by their relatively small dimensions and maintenance costs.

danilo.giulietti@unipi.it